Kinect V2 for Upper Limb Rehabilitation Applications
A Preliminary Analysis on Performance Evaluation

Giorgia Lupinacci, Gianluca Gatti, Agostino Angilica and Maurizio Muzzupappa

Dept. of Mechanical, Energy and Management Engineering (DIMEG), University of Calabria,
V. P. Bucci, Arcavacata di Rende (CS), 87036, Italy

Keywords: Upper Limb Rehabilitation, Upper Limb Joints Tracking, Kinect V2.

Abstract: Many systems have been developed to facilitate upper limb rehabilitation procedures in human subjects affected by trauma or pathologies and to retrieve information about patient performance. The Microsoft Kinect sensor can be used in this context to track body motion and detect objects. In order to evaluate the usability of this device in the upper limb rehabilitation field, a comparison with a marker-based system is presented in this paper. The upper limb motion is specifically considered and the performance on its detection and tracking is evaluated. The effect of the relative location between the Kinect and the observed subject is also investigated through experimental tests performed in different configurations.

1 INTRODUCTION

Modern upper limb rehabilitation systems use motion tracking technologies to evaluate patient performance, to aid limb motion in robotic assisted rehabilitation techniques or to allow interaction with virtual reality (Zhou and Hu, 2008). Shoulder, elbow and wrist joints tracking, is a necessary step for motion classification and recognition (Pimentel do Rosàrio, 2014). Furthermore, upper limb tracking allows to develop patient-specific therapies and is used to create serious games that induce motor recovery in a stimulating environment (Burke et al., 2009). Assisted motion control is also fundamental for the application of autonomous or semi-autonomous systems for motor recovery and to make rehabilitative experience possible at home (Prieto et al., 2014). Marker-less motion tracking systems for gaming are proposed as an alternative to marker-based systems (Moeslund et al., 2006; Lange et al., 2011) (usually adopted for motion analysis), because they are easy to use and less expensive. Moreover, a marker-less system is more flexible, because it offers the advantage to be used in several environments and configurations.

One of the most interesting marker-less systems available nowadays is the Microsoft Kinect™ (Kinect for Windows features, 2015). The device is able to retrieve the position of 25 human body joints and track up to six human subjects at the same time.

It predicts the body joints from a single depth image. From July 2014 a new version of the sensor is available, namely the Kinect for Windows v2.0, with improved performances respect to the first release, thanks to the higher fidelity of depth images (Lachat et al., 2015).

Kinect performance was studied using three main approaches: posture detection (Clark et al., 2012; van Diest et al., 2014; Diego-Mas and Alcaide-Marzal, 2014), joints centre evaluation (Xu and McGorry, 2015) and angles evaluation (Bonnechère et al., 2014; Chang et al., 2012). In particular, Xu and McGorry (Xu and McGorry, 2015) very recently proposed a comparison between the first and second generation of the Kinect and a marker-based system, concluding that no impressive improvements are introduced by the new version of the Kinect if the tracking is assessed at the whole skeleton level for static posture evaluation.

It is to be noted, however, that most of the available studies consider only the first generation of the Kinect (Bonnechère et al., 2014; Chang et al., 2012; Clark et al., 2012; van Diest et al., 2014), so the advantages of the second generation are not completely addressed, especially in the upper limb rehabilitation field.

The aim of this work is thus to validate the reliability of the second generation of the Kinect when adopted for upper limb rehabilitation. The study was conducted by taking into consideration (i)

the possibility to use the sensor in different positions without calibration and (ii) the body tracking algorithm, already integrated in the Kinect software. A marker-based system was used to conduct the evaluation of the upper limb tracking performance. The upper limb motion was executed by an healthy subject guided by the use of a specific end-effector as to emulate the movements usually asked to the patient during a robot-assisted rehabilitative session, e.g. the "reaching" and the "side to side" exercise (Volpe et al., 2008; Frisoli et al., 2012; Lam et al., 2008). The performances of the Kinect are compared to that of a marker-based system, for specific complex movements, affecting both the shoulder and elbow rotation simultaneously.

2 MATERIALS AND METHODS

Upper limb tracking was performed using the second version of the Microsoft Kinect for Windows and a stereo-photogrammetric optical system, the Optitrack (NaturalPoint, Inc. - Optical Tracking Solutions, 2015), consisting of 8 Flex13 cameras acquiring up to a frequency of 120 Fps. For body tracking, the Kinect body model and joints position were obtained from the associated Software Development Kit (SDK) v2.0 (Microsoft, Kinect for Windows, 2015), working at up to 30 Fps. For the Optitrack system, the NatNet SDK v2.7 (Natural Point Inc. - Optical Tracking Solutions, 2015) and the Motive 1.7.5 software (Natural Point Inc. - Optical Tracking Solutions, 2015) was adopted to capture the body joints position in conjunction with a motion capture suit and reflective markers. Figure 1 shows the set up for the upper limb tracking. In the figures both the Kinect sensor and the Optitrack cameras are indicated, as well as the corresponding coordinate systems used to retrieve numerical values.
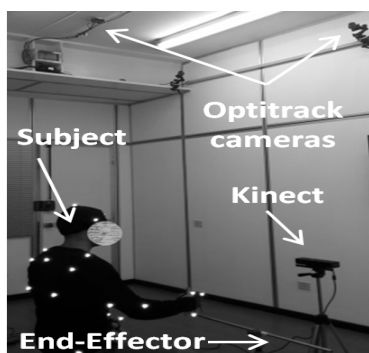

Figure 1: Experimental setup for upper limb tracking.

2.1 Upper Limb Tracking

During the study presented in this work, it was asked an healthy subject to make a set of movements using a passive end-effector. In particular, the end-effector which was visible in Figure 1 and is now shown in the detail of Figure 2, consisted of a tripod and a bar fixed on it. It was made to constrain the hand movement of the subject to a circular or a linear motion, so that a reference trajectory was available for validation. Each session was recorded by using both the Kinect and the Optitrack system.
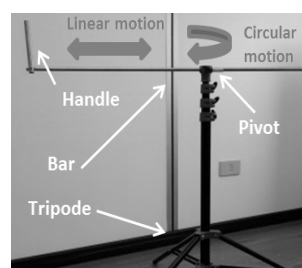

Figure 2: End-effector used for upper limb motion. It consists of a tripod and a bar.
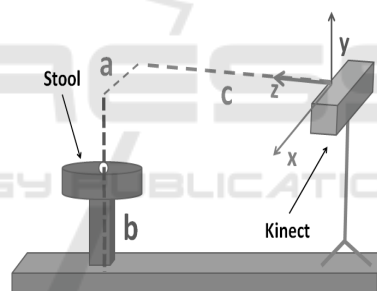

Figure 3: Schematic representation of Kinect position relative to the subject for upper limb tracking. Parameters are given in Table 1.

The healthy subject was seated on a stool, placed in the field of view of the Optitrack cameras and the Kinect was placed in six different positions as illustrated in Figure 3, but oriented so as it was facing the stool. The different positions where the Kinect was located are defined to be at the right, middle and left position relative to the axis orthogonal to the subject front plane, as defined in Table 1. For each of these positions, the Kinect was located at two different distances from the floor, respectively at about 800 mm and 1500 mm. In Table 1 these positions are summarized and labeled from K1 to K6 for ease of reference. The subject was wearing a motion capture suit with reflective markers to identify the shoulder, elbow and wrist joint, as shown in Figure 1. Such analysis is

performed to investigate if the Kinect position relative to the subject was somehow affecting the overall tracking procedure. A circular motion and a linear motion were thus executed by the right hand of the healthy subject for each position of the Kinect, as described above. It is worth noting that the healthy subject was asked not to rotate the wrist during the constrained motion, even if some small effect due to this compliant requirement are expected to affect the obtained results reported in Section 3.
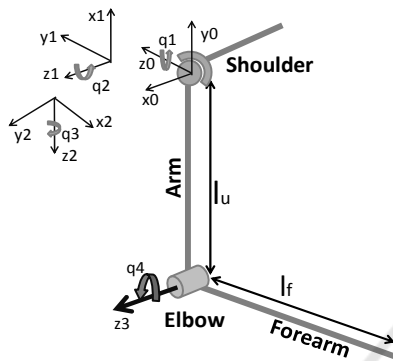

Figure 4: Schematic model of the upper limb with geometric parameters and joints variable, as defined in (Mihelj, 2006).

Table 1: Definition of the six Kinect position used for upper limb tracking.

Position	a [mm]	b[mm]	c [mm]
K1 – right down	800	800	-2000
K2 – right up	800	1500	-2000
K3 – middle down	0	800	-2000
K4 – middle up	0	1500	-2000
K5 – left down	-800	800	-2000
K6 – left up	-800	1500	-2000

The Kinect and the Optitrack frames were synchronized using the timestamp for direct comparison.

To determine the shoulder and elbow angles from the coordinates of the position of the shoulder, elbow and wrist joints obtained from the two optical systems, a 4 degree-of-freedom (DOF) inverse kinematic model of the human arm was used (Mihelj, 2006). A schematic model of the upper limb with geometric parameters is represented in Figure 4. The shoulder is modeled as a ball-and-socket joint with rotation axis for abduction-adduction (angle q_1), flexion-extension (angle q_2) and internal-external rotation (angle q_3).

With reference to Figure 4, l_u and l_f are, respectively, the arm and forearm lengths. The RMSDs between Optitrack angles variation and

Kinect angles variation were computed, to give an indication of the difference between the two systems.

The trajectory described by the wrist as computed from the two optical system for each session, is also used to assess the performance of the two motion tracking systems. In particular, a best-fit plane was determined on the set of points corresponding to the wrist position during motion. This is because the motion constrained by the end-effector was planar and this allowed to preliminary filter the results. Once projected on the corresponding best-fit plane, a second fitting was performed on the projected trajectories to fit a circle and a line, respectively, for the circular motion and for the linear motion of the hand grasping the end-effector. The RMSD of the residual errors of each fitting procedure, the radius of the fitted circle and the range of motion (RoM) for each trajectory were computed.

3 RESULTS

For upper limb tracking, the shoulder and elbow angles are computed for each of the 12 sessions (one circular and one translational motion for the six Kinect configurations). The sample in Figure 5 represents the results relative to the circular motion executed by the participant using the end-effector, with the Kinect at the middle down position K3, as defined in Table 1. In Figure 5(a-d) the variation of the angles $\Delta q_1, \ldots \Delta q_4$, are respectively showed, as obtained from the Kinect and Optitrack joints data, for a circular motion of the end-effector with the Kinect in position K3. Also, in Figure 5(e) the trajectories computed using the Kinect and the Optitrack data are showed.

Figure 6 illustrates the same information represented in Figure 5, but relative to a circular motion captured with the Kinect at the right down position K1, as defined in Table 1. Figure 7 and Figure 8 represent the results relative to the linear motion with the Kinect at the middle down position K3 and at the right down position K1, respectively.

It is worth noting that the parameters of the Kinect and Optitrack body model do not correspond to each other, and this is because of the intrinsic identification of joints location performed by the two systems. This means, in particular, that the arm and forearm length, as identified by the systems, are in general different, and they also vary along the acquisition time. For the Kinect, the identified joints location are affected mainly by the intrinsic system

setting, ambient light and sensor resolution. For the Optitrack, they are affected mainly by the body suit and the reflective marker location. To have a better insight into these effects, Table 2 and 3 reports the mean and STD of l_u and l_f as identified by the two optical systems, for the circular and linear motion of the end-effector, respectively.

Comparing Figure 5 to Figure 6, it can be seen that a better match between Optitrack and Kinect data is achieved for the first dataset. Furthermore, the wrist trajectory computed by the Kinect (Figure 6 (e)) presents some noise due to the high variation in the identification of the forearm and arm lengths, as explained above. In particular, from Table 2, it is observed that the STDs of l_u and l_f obtained by the Kinect at the middle down pose (K3), are the lowest compared to all the Kinect acquisitions. The STD of l_u when the Kinect is in position K5 is lower than for K3 but the STD of l_f is greater than for K3. The same observations can be done comparing Figure 7 and Figure 8. In the middle down configuration, indeed, the subject was completely visible and no joints occlusion occurred during the acquisitions.

In Table 4 and Table 5 the RMSDs obtained from the angles variations of the Optitrack and Kinect data are reported, for circular motions and linear motions, respectively. The lower trend of these values for middle positions (K3 and K4) of the Kinect confirms that this is the preferable position for the sensor. Tables 6 and 7 summarize the results obtained in terms of the wrist trajectory for the circular and linear motion, respectively. In Table 6 the radius associated to each circular trajectory after circle fitting, and the RoM are reported, while for the linear motion the RoM is reported in Table 7.

Table 2: Mean value μ of the arm length l_u, and forearm length l_f identified by the two optical systems along the acquisition frames, for the circular motion and for the different Kinect positions as from Table 1. The value in parenthesis is the STD (σ) of the correspondent distribution. The sub-script "K" stands for Kinect, while the "O" stands for Opitrack.

		Circular Motions					
		K1	**K2**	**K3**	**K4**	**K5**	**K6**
l_u [mm]	μ_K (σ)	280.6 (12.6)	204.6 (18.0)	202 (4.4)	224.6 (20.5)	188.1 (2.3)	230.7 (10)
	μ_O (σ)	286.0 (6E-4)	286.0 (7E-4)	276.5 (4E-3)	286 (1E-3)	286 (1E-3)	286 (8E-4)
l_f [mm]	μ_K (σ)	234 (3)	213.5 (18.3)	203.6 (0.8)	215.3 (11.2)	192 (11.1)	223 (8.6)
	μ_O (σ)	285 (7.2)	275.4 (12.0)	252.0 (12.5)	263.2 (9.4)	253.3 (2)	268.5 (9.2)

Table 3: Mean value μ of the arm length l_u, and forearm length l_f identified by the two optical systems along the acquisition frames, for the circular motion and for the different Kinect positions as from Table 1. The value in parenthesis is the STD (σ) of the correspondent distribution. The sub-script "K" stands for Kinect, while the "O" stands for Opitrack.

		Linear Motions					
		K1	**K2**	**K3**	**K4**	**K5**	**K6**
l_u [mm]	μ_K (σ)	230.5 (11.5)	222.4 (7.7)	248 (4.1)	211 (19.4)	243.5 (6.8)	230.7 (10)
	μ_O (σ)	286.0 (1E-3)	286 (4E-4)	286 (6E-4)	286 (4E-4)	286 (4E-4)	285.8 (9E-4)
l_f [mm]	μ_K (σ)	239.7 (25.3)	216.0 (7)	187.5 (1.6)	232.6 (16.3)	222 (7.2)	223 (8.5)
	μ_O (σ)	274.0 (4.4)	260.4 (8.4)	236.0 (8.2)	243.6 (7.5)	268.2 (14)	268.5 (9.2)

Table 4: RMSDs obtained comparing the arm angles variations for Kinect and Optitrack for the circular motions of the end-effector and for the six different Kinect configurations from Table 1.

	Circular Motions					
	K1	**K2**	**K3**	**K4**	**K5**	**K6**
RMSD Δq_1	2.5	32.2	6	1.1	5.7	3
RMSD Δq_2	2.0	10.6	3.1	4.5	5.7	4
RMSD Δq_3	20.0	53.0	21.2	4.0	2.6	31
RMSD Δq_4	4.9	17.8	8.4	11.8	3.6	2.7

Table 5: RMSDs obtained comparing the arm angles variations for Kinect and Optitrack for the linear motion of the end-effector and for the six different Kinect configurations from Table 1.

	Linear Motions					
	K1	**K2**	**K3**	**K4**	**K5**	**K6**
RMSD Δq_1	17.05	7.4	6.7	7.9	3.8	6.7
RMSD Δq_2	16.1	9.2	4.5	1.1	4.5	1.8
RMSD Δq_3	27.7	7.6	8.5	6.0	20.4	32.0
RMSD Δq_4	16.4	5.7	8.4	4.4	7.7	3.7

Table 6: Results of the wrist trajectories for circular motion. Circle-fitted radius and estimated RoM, for the six different Kinect configurations as from Table 1. The "K" stands for Kinect and the "O" stands for Optitrack.

		K1	**K2**	**K3**	**K4**	**K5**	**K6**
Radius [mm]	K	180	102	95.6	118	122	183
	O	179.1	163.3	119.6	201.4	198.7	176.5
RoM [deg]	K	105.2	111.7	129.0	96.5	114.3	148
	O	92.3	102.1	121.3	76.8	111.8	173.3

Table 7: Results of the wrist trajectories for linear motion. Estimated RoM, for the six different Kinect configurations as from Table 1. The "K" stands for Kinect and the "O" stands for Optitrack.

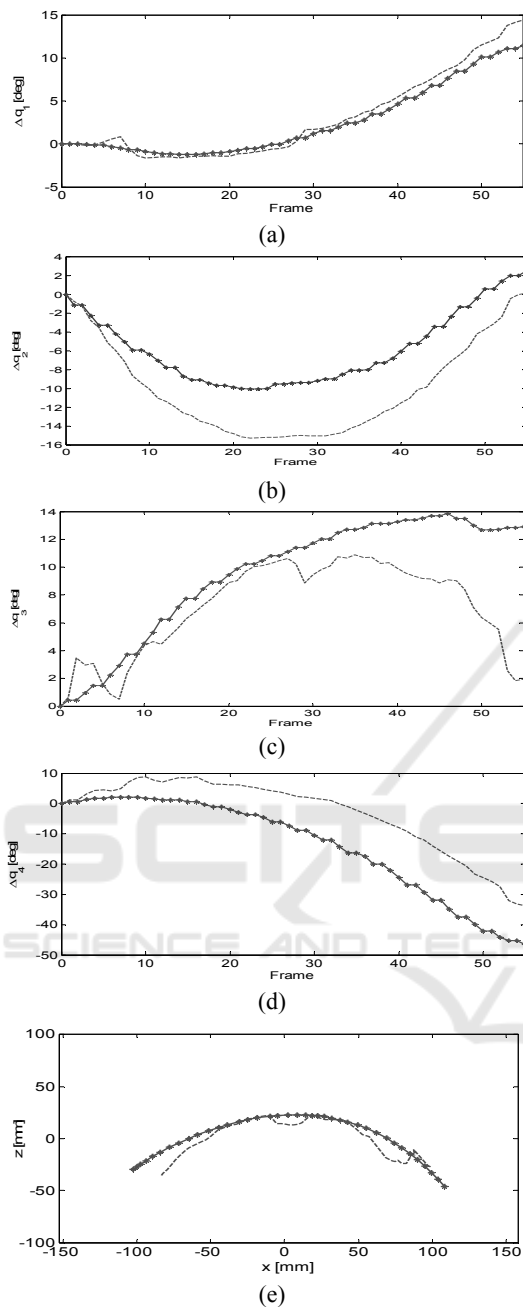|		**K1**	**K2**	**K3**	**K4**	**K5**	**K6**
RoM [mm]	K	234.2	240	263.4	228.5	273.3	293.8
	O	312.2	326	284.9	308.6	292.2	316.9

(a)

(b)

(c)

(d)

(e)

Figure 5: Results for the circular motion of the end-effector using the right arm, with Kinect in position K3. (a) Δq_1, (b) Δq_2, (c) Δq_3, (d) Δq_4, (e) estimated wrist trajectory by Optitrack (spotted lines) and Kinect (discontinue lines). The axes x and z represent the coordinates of the best-fit plane determined on the set of points corresponding to the wrist position during motion.

For the circular motions, the mean value of the difference between the radius of the circle fitted on the Kinect data and on the Optitrack data is 42(36) mm, where the value in parentheses represents the
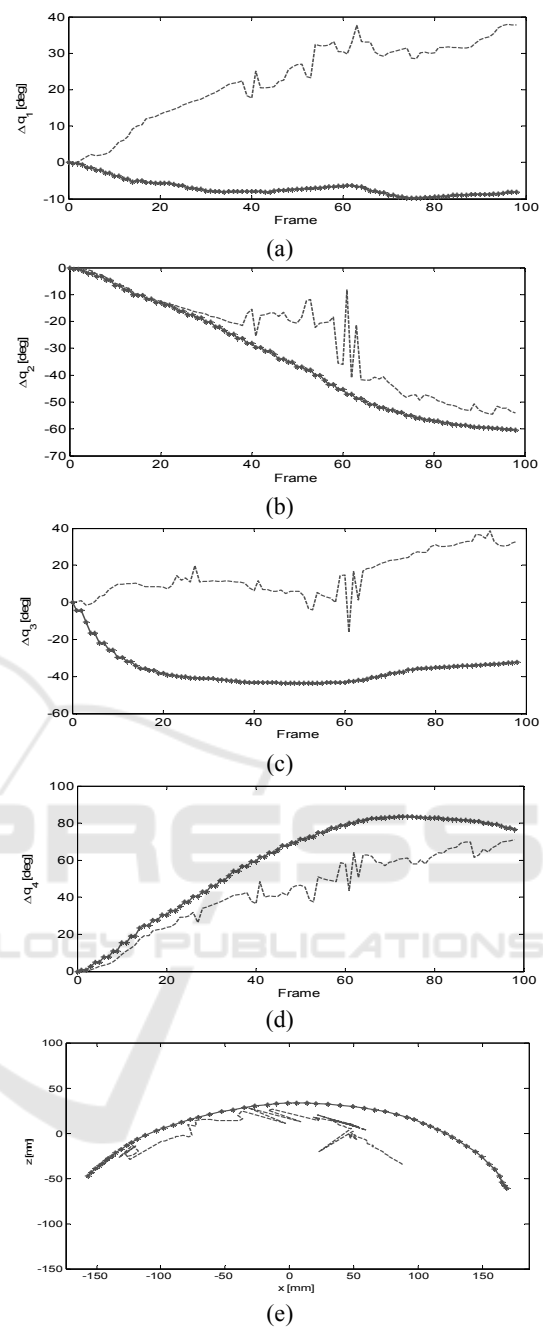

(a)

(b)

(c)

(d)

(e)

Figure 6: Results for the circular motion of the end-effector using the right arm, with Kinect in position K2. (a) Δq_1, (b) Δq_2, (c) Δq_3, (d) Δq_4, (e) estimated wrist trajectory by Optitrack (spotted lines) and Kinect (discontinue lines). x and z are the coordinate of the best-fit plane determined on the set of points corresponding to the wrist position during motion.

STD of the correspondent distribution. Instead, the mean difference between the ROM computed from the Kinect data and from the Optitrack data, is 13(8.3) deg. Finally, the mean difference between
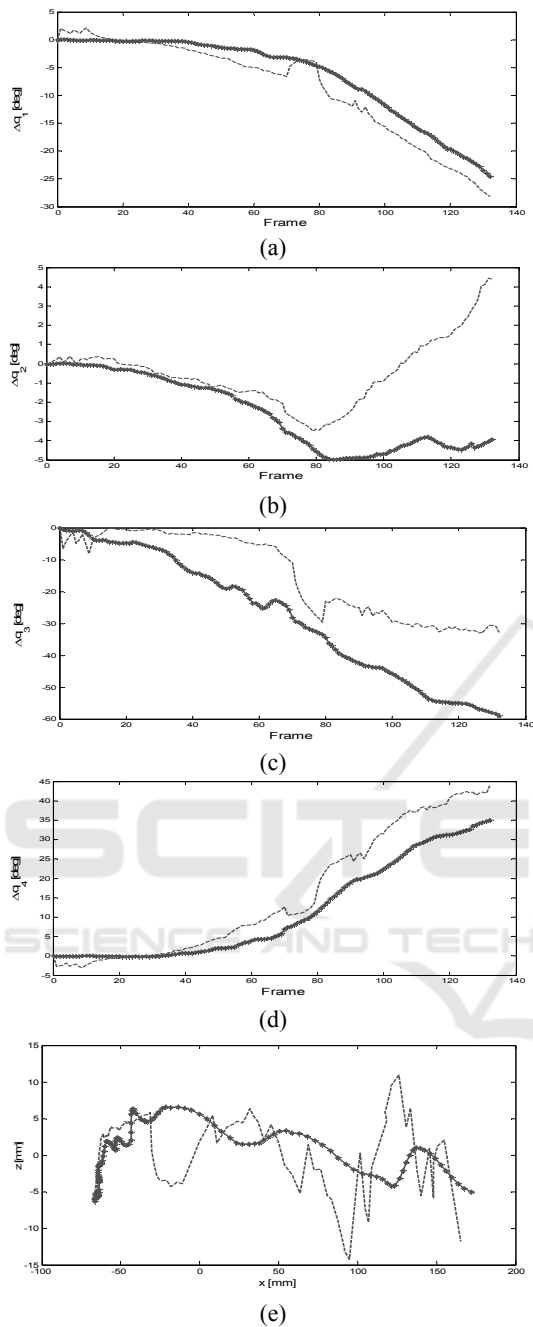
135

(a)

(b)

(c)

(d)

(e)

Figure 7: Results for the linear motion of the end-effector using the right arm, with Kinect in position K3. (a) Δq_1, (b) Δq_2, (c) Δq_3, (d) Δq_4, (e) estimated wrist trajectory by Optitrack (spotted lines) and Kinect (discontinue lines). The axes x and z represent the coordinates of the best-fit plane determined on the set of points corresponding to the wrist position during motion.

the ROM on the linear motion of the hand on the bar is equal to 51.4(33.3) mm.

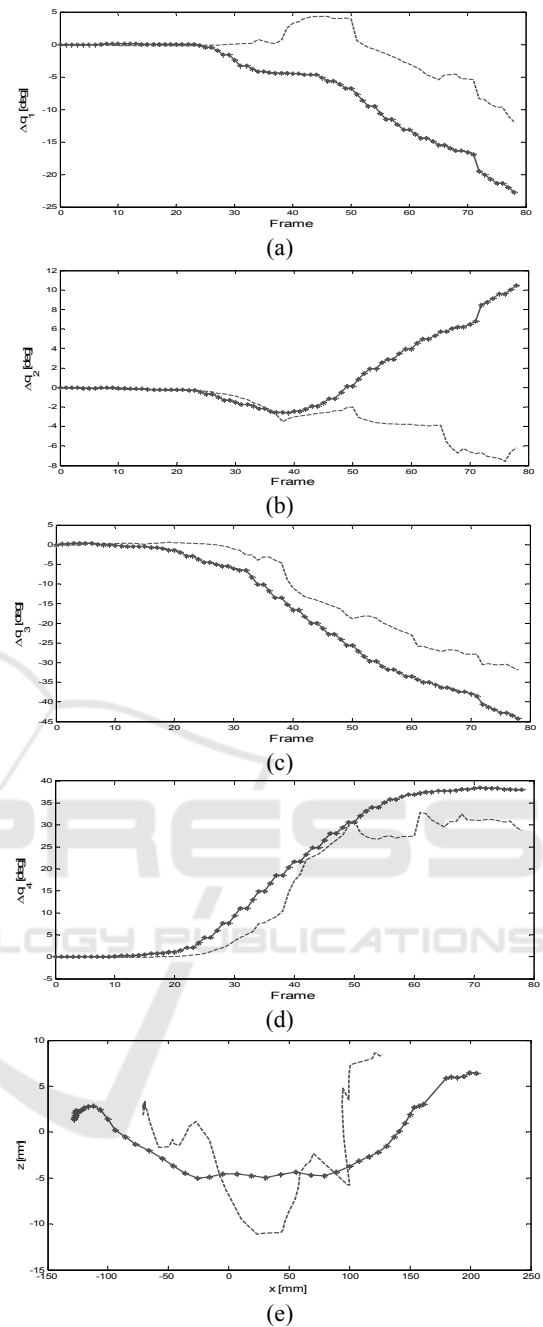From Figures 5, Figure 6, Figure 7 and Figure 8

(a)

(b)

(c)

(d)

(e)

Figure 8: Results for the linear motion of the end-effector using the right arm, with Kinect in position K2. (a) Δq_1, (b) Δq_2, (c) Δq_3, (d) Δq_4, (e) estimated wrist trajectory by Optitrack (spotted lines) and Kinect (discontinue lines). x and z are the coordinate of the best-fit plane determined on the set of points corresponding to the wrist position during motion.

it is seen that there are some offsets between the angles estimated by the two systems, and this is due to the different body model inherently adopted by

the Kinect and Optitrack, as discussed above. For this reason it is not expected that the angles obtained from the data captured by the two systems are the same. The comparison between the two systems in terms of RoM should be then taken as a qualitative indication only.

4 DISCUSSION

This paper presented a preliminary investigation on the expected results and performance that could be obtained when using the marker-less Kinect sensor for upper limb motion tracking, with specific application to the rehabilitation of the upper limb. In particular, the aim of this study was focused on the Kinect v2, recently released by the Microsoft. An auxiliary marker-based Optitrack system, composed by 8 cameras and motion capture suit with reflective markers, was used as reference. The Kinect marker-less system can be used to detect objects in the 3D space with an accuracy close to the centimetre (Lachat et al., 2015). The accuracy of the Optitrack system has been estimated to be of the order of the millimetre (Carse et al., 2013). So, the Optitrack system exhibits an accuracy higher than that of the Kinect, and this confirm its use as a reference.

For the upper limb tracking procedure, a realistic experimental setup was created. An healthy subject (participant) was asked to execute specific motions grasping an end-effector, in order to reproduce a robotic-assisted rehabilitation procedure (Zhou and Hu, 2008). It was observed that, in order to have a better precision and accuracy, the Kinect should be located in front of the subject. The comparison between the two optical systems could only give qualitative indication on the relative precision and accuracy in detecting upper limb tracking. This was related to the inherently different body models implemented in the Kinect and Optitrack software tools. Furthermore, on the one hand the Optitrack data were affected by the presence of the body suit, its fitting to the participant, and by the location and observability of the reflective markers. On the other hand, the Kinect data were mainly affected by the ambient lightning and by the lower resolution of the sensors.

To check the reliability of the body model data, the mean and STD of both the arm and forearm, as identified by the two optical systems along the acquired frames are calculated. It is shown that, when the Kinect is located in front of the subject, the deviations relative to the arm and the forearm lengths computed by the Kinect were lower, as to suggest that the device is more precise in such configuration rather than in others, where it is inclined respect to the subject. However, the results obtained when the Kinect was in these latter configurations do not dramatically exclude their usability for a qualitative evaluation of the upper limb motion. It was also observed that, if the upper body of the subject is completely in the field of view of the Kinect and no occlusion of the joints occurs during motion, the body tracking allows to approximate the trajectory of the wrist with lower noise. However, the estimate of the joints position is not accurate, as suggested by the STD of segments length computed using the Kinect data. Indeed, comparing the Kinect data with the Optitrack data, as reported in Table 2, it is possible to note that, for every acquisition step, the Optitrack identifies the length of the upper arm with a very low STD, whereas the Kinect gives different mean lengths for each acquisition step. For the Optitrack data, the mean length of the forearm results to be variable for each acquisition step because of the motion tracking suit, particularly at the wrist.

5 CONCLUSIONS

This preliminary study suggested that the Kinect may be potentially adopted for applications involving upper limb rehabilitation. The advantages of such a system are the low cost, no requirement for calibration, the easy to use and to set up, and the absence of any body marker or suit that could inevitably involve motion artefact. However, the main limitation is the lower resolution, compared to the more expensive marker-based systems. Nevertheless, such resolution, of about few tens of millimetres for the experimental test performed here on the upper limb, make the Kinect an interesting tool for applications in the rehabilitation field.

Future works are aimed at carrying out a more detailed and extensive experimental analysis involving several healthy subjects with different characteristics, trying to come up with a more reliable statistical analysis and some concluding evidence on the usability of the device for the specific body application.

REFERENCES

Asín Prieto G., Cano-de-la-Cuerda R., López-Larraz E., Metrot J., Molinari M., van Dokkum, L. E. H., 2014. Emerging Perspectives in Stroke Rehabilitation. In

Emerging Therapies in Neurorehabilitation Biosystems & Biorobotics, vol. 4, pp 3-21. SPRINGER.

Beucher, S., 1992. The watershed transformation applied to image segmentation. *In Scanning Microscopy-Supplement-, pp 299-299*.

Bonnechère, B., Jansen, B., Salvia, P., Bouzahouene, H., Omelina, L., Moiseev, F., Sholukha, V., Cornelis, J., Van Sint Jan, S., 2014. Validity and reliability of the Kinect within functional assessment activities: Comparison with standard stereophotogrammetry. In *Gait & Posture, vol. 39, no.1, pp 593 – 598.* ELSEVIER.

Burke, J. W., McNeill, M. D. J., Charles, D. K., Morrow, P. J., Crosbie, J. H., McDonough, S. M., 2009. Optimising engagement for stroke rehabilitation using serious games. In *The Visual Computer, vol.12, no. 25, pp 1085-1099.* SPRINGER.

Carse, B., Meadows, B., Bowers, R., Rowe, P., 2013. Affordable clinical gait analysis: An assessment of marker tracking accuracy of a new low-cost optical 3D motion analysis system. In *Physiotherapy, vol. 99, no. 4, pp347-351.* ELSEVIER.

Chang,C.-Y., Lange, B., Zhang, M., Koenig, S., Requejo, P., Somboon, N., Sawchunk, A.A., Rizzo, A.A., 2012. Toword pervasive physical rehabilitation using Microsoft Kinect. In *2012 6th International Conference on Pervasive Computing Technologies for Healthcare and Workshops, PervasiveHealth 2012, pp 159-162.*

Clark, R.A., Pua, Y., Fortin, K., Ritchie C., Webster, K.E., Denehy, L., Bryant, A.L., 2012. Validity of the Microsoft Kinect for assessment of postural control. In *Gait & Posture, vol. 36, no.3, pp 372-577.* ELSEVIER.

Diego-Mas, J. A., Alcaide-Marzal, J., 2014. Using Kinect^{TM} sensor in observational methods for assessing postures at work. *Applied Ergonomics, vol. 45, no.4, pp 976 – 985.* ELSEVIER.

Frisoli, A., Procopio, C., Chisari, C., Creatini, I., Bonofiglio, L., Bergamasco, M., Rossi, B., Carboncini, M. C., 2012. Positive effects of robotic exoskeleton training of upper limb reaching movements after stroke. In *Journal of Neuroengineering and Rehabilitation, vol. 9, no. 36. BioMed Central.*

Kinect for Windows features. Available from: https://www.microsoft.com/enus/kinectforwindows/meetkinect/features.aspx [3August 2015]

Lachat, E., Macher, H., Mittet M. A., Landes, T., Grussenmeyer, P., 2015. First experiences with Kinect v2 sensor for close range 3D modelling. In *The International Archives of the Photogrammetry, Remote Sensing and Spatial Information Sciences, Volum XL-5/W4.*

Lam, P., Hebert, D., Boger, J., Lacheray, H., Gardner, D., Apkarian, J., Mihailidis, A., 2008. A haptic-robotic platform for upper-limb reaching stroke therapy: preliminary design and evaluation results. In *Journal*

of Neuroengineering and Rehabilitation, vol. 5, no. 15. BioMed Central.

Lange, B., Chang, C., Suma, E., Newman, B., Rizzo, A., Bolas, M., 2011. Development and evaluation of low cost game-based balance rehabilitation tool using the Microsoft Kinect sensor. In *Engineering in Medicine and Biology Society, EMBC, 2011 Annual International Conference of the IEEE, pp 1831-1834. IEEE.*

Mihelj, M., 2006. Human Arm Kinematics for Robot Based Rehabilitation. In *Robotica, vol. 24, no. 3, pp 377-383.* CAMBRIDJE UNIVERSITY PRESS.

Moeslund, T. B., Hilton, A., & Krüger, V., 2006. A survey of advances in vision-based human motion capture and analysis. In *Computer vision and image understanding, vol. 104, no. 2, pp 90-126.* ELSEVIER.

Natural Point, 2015. Inc.: Optitrack-optical motion tracking solutions. Available from: https://www.naturalpoint.com/.

Pimentel do Rosàrio, J.L., 2014. Biomechanical assessment of human posture: A literature review. In *Journal of Bodywork and Movement Therapies, vol.18, no. 3, pp 368-373.* ELSEVIER.

Van Diest, M., Stegenga, J., Heinrich, J.W., Postema K., Verkerke, G. J., Lamoth, C. J. C., 2014. Suitability of Kinect for measuring whole body movement patterns during exergaming. *Journal of Biomechanics, vol. 47, no.12, pp 2925 – 2932.* ELSEVIER.

Volpe, B. T., Lynch, D., Rykman-Berland, A., Ferraro, M., Galgano, M., Hogan, N., Krebs, H.I., 2008. Intensive Sensorimotor Arm Training Mediated by Therapist or Robot Improves Hemiparesis in Patients With Chronic Stroke. In *Neurorehabilitation & Neural Repair, vol. 22, no. 3, pp 305-310. SAGE.*

Xu, X., McGorry, R. W., 2015. The validity of the first and second generation Microsoft Kinect^{TM} for identifying joint center locations during static postures. In *Applied Ergonomics, vol. 49, pp 47 – 54.* ELSEVIER.

Zhou, H., Hu, H., 2008. Human motion tracking for rehabilitation-A survey. In *Biomedical Signal Processing and Control, vol.3, no. 1, pp 1-18.* ELSEVIER.